

¹ RGTFun: An Open-Source MATLAB App for Rarefied Gas Transport Coefficient Calculations

³ Jackson Granat¹, Nathan Bartlett¹, and David N. Ruzic¹

⁴ 1 Department of Nuclear, Plasma, and Radiological Engineering, The University of Illinois at
⁵ Urbana-Champaign, Urbana, Illinois 

DOI: [10.xxxxxx/draft](https://doi.org/10.xxxxxx/draft)

Software

- [Review](#) 
- [Repository](#) 
- [Archive](#) 

Editor: Pi-Yueh Chuang  

Reviewers:

- [@Stephen-Armstrong](#)
- [@drobnyjt](#)

Submitted: 05 March 2025

Published: unpublished

License

Authors of papers retain copyright
and release the work under a
Creative Commons Attribution 4.0
International License ([CC BY 4.0](#))

⁶ Key Definitions

- ⁷ b - impact parameter (\AA)
- ⁸ θ_c - center of mass scattering angle (radians)
- ⁹ r_o - distance of closest approach during a binary elastic collision (\AA)
- ¹⁰ r_m - location of the energy minimum of the intermolecular potential (\AA)
- ¹¹ ϵ - the depth of the attractive portion of the intermolecular potential (eV)
- ¹² D_{12} - the binary diffusion coefficient ($\text{m}^2 \cdot \text{s}$)
- ¹³ μ - viscosity coefficient ($\text{Pa} \cdot \text{s}$)
- ¹⁴ E_c - center of mass energy during a collision (eV)
- ¹⁵ E_l - lab frame energy (eV)
- ¹⁶ $\sigma(\theta_c)$ - the differential scattering cross section
- ¹⁷ σ_T - total cross section (m^2)
- ¹⁸ σ_D - the diffusion cross section, also called the momentum cross section (m^2)
- ¹⁹ σ_μ - the viscosity cross section (m^2)
- ²⁰ r - distance between the centers of two molecules (\AA)
- ²¹ $U(r)$ - the intermolecular potential energy function of two molecules (eV)
- ²² S - the stopping cross section ($\text{eV} \cdot \text{m}^2 \cdot \text{molecule}^{-1}$)
- ²³ χ - $(\pi - \theta_c)/2$
- ²⁴ Z_1 - number of protons of the first colliding molecule
- ²⁵ Z_2 - number of protons of the second colliding molecule
- ²⁶ q - elementary charge (C)
- ²⁷ d_{ref} - the reference diameter of the collision model used in the variable hard sphere model
incorporated into the direct simulation Monte-Carlo method (\AA)
- ²⁸ ω - the DSMC viscosity temperature dependence parameter
- ²⁹ N_a - Avogadro's number (atoms / mol)
- ³⁰ P_{vap} - equilibrium vapor pressure (Pa)
- ³¹ k_B - Boltzmann's constant ($J \cdot K^{-1}$)
- ³² T - temperature (K)
- ³³ d_{12} - collision diameter used in the VHS collision rule for DSMC simulations
- ³⁴ VHS - variable hard sphere - the collision rule used for the DSMC

³⁶ Statement of Need

³⁷ RGTFun is a MATLAB app designed for the efficient calculation of scattering integrals and
³⁸ transport coefficients of elastic collisions. While the solution for classical scattering, as well as
³⁹ its application for determining gas transport coefficients, has been known for over approximately
⁴⁰ a century ([Chapman & Cowling, 1990](#)), the numerical codes are usually kept as closed-source
⁴¹ or are printed in textbooks in older programming languages such as FORTRAN ([Maitland,](#)

42 1987). To our knowledge, existing publicly available tools (e.g., MagnumPI for calculation of
43 scattering angles and cross sections (Janssen, 2018); SRIM for stopping power calculations
44 (James F. Ziegler et al., 2010)) offer limited support for user-adjustable interatomic potentials
45 (especially across energy regimes) in end-to-end workflows that compute scattering integrals
46 and the resulting transport coefficients.

47 RGTFun is open-source and implemented in MATLAB, leveraging its numerical computing
48 capabilities and App Designer for the graphical interface. Furthermore, the code features a
49 well-designed graphical user interface (GUI) to facilitate the step by step process of going
50 from an intermolecular potential to macroscopic transport coefficients such as viscosity and
51 diffusion coefficients. The ethos of the project is to decrease the learning curve of going from
52 quantum chemistry calculations of intermolecular potential energy surfaces to usable transport
53 coefficients in CFD or PIC codes.

54 State of the Field

55 The closest existing open-source tool to RGTFun is MagnumPI, which focuses on computing
56 scattering angles, cross sections, and collision integrals for several (but not all) intermolecular
57 potentials (Janssen, 2018). SRIM is widely used for stopping power calculations, but it is not
58 designed to calculate transport coefficients and does not support user-adjustable interatomic
59 potentials in the manner required here (James F. Ziegler et al., 2010).

60 We chose to develop RGTFun rather than contribute to existing tools because our target use
61 case requires capabilities beyond collision-scale quantities: RGTFun computes macroscopic
62 transport coefficients (e.g., viscosity and diffusion) and also provides simplified collision-model
63 parameters for variable hard sphere (VHS) and variable soft sphere (VSS) models. In addition,
64 RGTFun is organized as an end-to-end, user-guided workflow with intermediate diagnostics
65 (e.g., distance of closest approach) to help users verify expected behavior at each stage. This
66 combination of user-adjustable potentials across energy regimes, end-to-end transport outputs,
67 and a validation-oriented GUI fills a gap not addressed by existing open-source tools.

68 Research Impact Statement

69 RGTFun has been incorporated into the authors' computational workflow to generate coefficients
70 for downstream modeling. By providing an end-to-end workflow from an intermolecular potential
71 to macroscopic transport coefficients (e.g., viscosity and diffusion), RGTFun lowers the barrier
72 for translating potential energy surfaces from quantum chemistry into inputs for CFD or PIC
73 simulations. In addition to interactive GUI use, the modular scripts support batch execution
74 for parameter sweeps and integration into existing pipelines. The validation cases in this
75 paper provide a reference analysis spanning analytic scattering, screened-potential benchmarks,
76 cross-tool comparison to SRIM, and comparison to NIST transport data.

77 Software Design

78 RGTFun was designed around three principles: (i) provide a user-friendly graphical interface
79 that guides users through computing scattering quantities and transport coefficients from
80 interatomic potentials, (ii) build on established formulations and numerical methods from
81 the literature rather than introducing new theory, and (iii) support both interactive use and
82 reproducible, scriptable workflows.

83 A central architectural decision was to implement RGTFun as a multi-tab MATLAB App
84 Designer application, where each tab corresponds to a major stage of the workflow (e.g.,
85 defining the interatomic potential, computing cross sections, evaluating scattering integrals, and
86 computing transport coefficients). This structure mirrors how users validate these calculations

in practice: each stage produces intermediate plots and diagnostics so the user can verify expected behavior before proceeding. The trade-off is that the GUI adds some maintenance overhead compared to a single end-to-end script, but it reduces user error and lowers the barrier to entry for new users.

MATLAB was selected primarily for MATLAB App Designer's extensive GUI toolbox and for performance in vectorized numerical computing. Choosing MATLAB also enabled direct reuse of the open-source Chebfun library for numerically robust and efficient root-finding when solving for the distance of closest approach, avoiding the need to reimplement specialized numerical routines and improving runtime performance.

A second key decision was to keep the computational core modular and usable without the GUI. Each major calculation step is implemented as an independent script/function that takes only two inputs: (1) a user-specified input file and (2) an output directory. The GUI serves as a front-end that generates or selects inputs, runs these core routines, and forwards output paths to downstream steps. This design supports advanced users who prefer command line execution, makes batch runs straightforward, and simplifies validation: benchmark input files can be run through individual calculation steps and compared against expected outputs.

Lastly, we built a rigorous testing suite that utilizes MATLAB's internal unit testing framework to test each script in RGTFun against reference data that is included with the app. We welcome issues and pull requests, and we encourage users to extend the app to their applications.

106 Theory

107 The Intermolecular Potential

108 The intermolecular potential describes the potential energy between two atoms or molecules
 109 and is a function of their distance r . The actual shape of the potential energy surface of two
 110 molecules is unique to the pair and determined using quantum chemistry software ([Valiev et al., 2010](#)) or experiments ([Amdur, 1961](#); [I. Amdur, 1949](#); [I. Amdur & Harkness, 1954](#); [Ruzic & Cohen, 1984](#)). RGTFun currently supports the following intermolecular potential models:

- 113 ▪ Coulomb Potential

$$U(r) = \frac{Z_1 Z_2 e^2}{4\pi\epsilon_0 r}$$

- 114 ▪ 12-6 Lennard-Jones Potential ([Lennard-Jones, 1931](#))

$$U(r) = 4\epsilon \left[\left(\frac{\sigma}{r} \right)^{12} - \left(\frac{\sigma}{r} \right)^6 \right]$$

115 where

$$\sigma = 2^{-1/6} r_m$$

- 116 ▪ 12-4 Lennard-Jones Potential ([Zhen & Davies, 1983](#))

$$U(r) = \frac{3^{3/2}}{2} \epsilon \left[\left(\frac{\sigma}{r} \right)^{12} - \left(\frac{\sigma}{r} \right)^4 \right]$$

117 where

$$\sigma = 3^{-1/8} r_m$$

- 118 ▪ ZBL Potential ([J. F. Ziegler et al., 1983](#))

$$U(r) = \frac{1}{4\pi\epsilon_0} \frac{Z_2 Z_2 e^2}{r} \phi(r/a)$$

¹¹⁹ where

$$a = \frac{0.46850}{Z_1^{0.23} + Z_2^{0.23}}$$

¹²⁰ and

$$\phi(x) = 0.18175e^{-3.19980x} + 0.50986e^{-0.94229x} + 0.28022e^{-0.40290x} + 0.02817e^{-0.20162x}$$

¹²¹ ▪ Morse Potential ([Morse, 1929](#))

$$U(r) = \epsilon \left(e^{-2a(r-r_m)} - 2e^{-a(r-r_m)} \right)$$

¹²² where

$$a = \sqrt{\frac{k}{2\epsilon}}$$

¹²³ ▪ Power Law Potential

$$U(r) = ar^{-k}$$

¹²⁴ Bimolecular Scattering

¹²⁵ Once an intermolecular potential is known, the scattering angle can be determined as a function
¹²⁶ of impact energy and impact parameter. First, the distance of closest approach r_o must be
¹²⁷ solved by finding the root of equation (1), where E_c is the center of mass energy. Next, the
¹²⁸ scattering angle θ_c is solved by integrating equation (2).

$$1 - \frac{V(r_o)}{E_c} - \frac{b^2}{r_o^2} = 0 \quad (1)$$

$$\theta_c = \pi - 2 \int_{r_o}^{\infty} \frac{b dr}{r^2 \sqrt{1 - \frac{V(r)}{E_c} - \frac{b^2}{r^2}}} \quad (2)$$

¹²⁹ Cross Sections

¹³⁰ With a relationship between the impact parameter and scattering angle, cross section quantities
¹³¹ can be defined. The differential cross section is defined by equation (3). The total cross
¹³² section is defined by equation (4). It is important to note that the classical cross section is
¹³³ infinite. If a quantum mechanical approach is taken, then the total cross section becomes
¹³⁴ finite again. Instead of doing a quantum mechanical calculation, we can instead define a cutoff
¹³⁵ angle, θ_{cutoff} , which has a corresponding cutoff impact parameter which makes a finite cross
¹³⁶ section according to equation (5). The cutoff angle can be chosen to either be the smallest
¹³⁷ measurable angle or when the classical scattering is no longer valid. The condition for the
¹³⁸ cutoff angle becoming invalid is given by equation (6) ([Lane & Everhart, 1960](#)). Solving
¹³⁹ equation (6) requires a numerical root finding procedure. The momentum cross section is
¹⁴⁰ given by equation (7) and the viscosity cross section is given by equation (8). These last two
¹⁴¹ cross sections are needed to calculate continuum transport coefficients using Chapman-Enskog
¹⁴² theory. The final cross section of importance is the stopping cross section, given by equation
¹⁴³ (9), which tells us how much energy is lost per unit travel per unit density.

$$\sigma(\theta_c, E) = \left| \frac{b}{\sin(\theta_c)} \frac{db}{d\theta} \right| \quad (3)$$

$$\sigma_T(E) = \int_0^\pi \sigma(\theta_c, E) 2\pi \sin(\theta_c) d\theta_c = 2\pi \int_0^\infty b db = \infty \quad (4)$$

$$\sigma_T(E)_{classical} = \int_{\theta_{cutoff}}^{\pi} \sigma(\theta_c, E) 2\pi \sin(\theta_c) d\theta_c = \int_0^{b_{cutoff}} b db = 2\pi b_{cutoff}^2 \quad (5)$$

$$\theta_c(b_{cutoff}) - \frac{\hbar}{2\sqrt{2E_c/m_r} \cdot r_o(b_{cutoff}, E_c)} = 0 \quad (6)$$

$$\sigma_D(E) = \int_0^{\pi} (1 - \cos(\theta_c)) \cdot \sigma(\theta_c, E) 2\pi \sin(\theta_c) d\theta_c = 2\pi \int_0^{\infty} (1 - \cos(\theta_c)) \cdot b db \quad (7)$$

$$\sigma_\mu(E) = \int_0^{\pi} (1 - \cos^2(\theta_c)) \cdot \sigma(\theta_c, E) 2\pi \sin(\theta_c) d\theta_c = 2\pi \int_0^{\infty} (1 - \cos^2(\theta_c)) \cdot b db \quad (8)$$

$$S_n = \frac{1}{n} \frac{dE}{dx} = \gamma E \sigma_D \quad (9)$$

¹⁴⁴ where

$$\gamma = \frac{2M_1 M_2}{(M_1 + M_2)^2}$$

¹⁴⁵ Continuum Transport Coefficients

¹⁴⁶ The binary diffusion and single species viscosity coefficient can be determined by using the
¹⁴⁷ results of Chapman-Enskog theory ([Chapman & Cowling, 1990](#); [Maitland, 1987](#)). The binary
¹⁴⁸ diffusion coefficient is given by equation (10) and the single species viscosity is given by
¹⁴⁹ equation (11). The collision integrals are calculated using the results of the cross sections
¹⁵⁰ discussed in the previous section.

$$D_{12} = \frac{3}{16} \cdot \left(\frac{2\pi k_B T (m_1 + m_2)}{m_1 m_2} \right)^{1/2} \frac{1}{n \overline{\Omega}_{12}^{(1,1)}} \quad (10)$$

$$\mu = \frac{5}{8} \cdot \left(\frac{2\pi k_B T (m_1 m_2)}{(m_1 + m_2)} \right)^{1/2} \frac{1}{\overline{\Omega}^{(2,2)}} \quad (11)$$

$$\overline{\Omega}_{12}^{(1,1)} = \frac{1}{2} (k_B T)^{-3} \int_0^{\infty} \sigma_D E^2 e^{-\frac{E}{k_B T}} dE \quad (12)$$

$$\overline{\Omega}^{(2,2)} = \frac{1}{2} (k_B T)^{-4} \int_0^{\infty} \sigma_\mu E^3 e^{-\frac{E}{k_B T}} dE \quad (13)$$

¹⁵¹ DSMC Coefficients

¹⁵² The most common DSMC collision rule is called the variable hard sphere (VHS) model. In
¹⁵³ this model, the relative velocity of two colliding particles determines an effective hard sphere
¹⁵⁴ potential and the particles collide according to the classic hard sphere scattering rule ([Bird,](#)
¹⁵⁵ [2013](#)). This rule is given by equation (14) where d_{12} is the average of the two particles'
¹⁵⁶ diameters and is a function of the relative velocity according to equation (15). The value of ω
¹⁵⁷ in equation (15) is determined by fitting viscosity data over a limited range of temperatures
¹⁵⁸ which passes through a reference viscosity, μ_{ref} , at a chosen reference temperature, T_{ref} ,
¹⁵⁹ according to equation (16). Note that equation (14), the hard shell scattering rule, is undefined
¹⁶⁰ at impact parameters larger than d_{12} which defines its total cross section ([Fratus, 2015](#)).

$$b = d_{12} \cdot \cos(\theta_c/2) \quad (14)$$

$$d_{12} = \left(\frac{15 \cdot \sqrt{mk_b T / \pi}}{2 \cdot (5 - 2\omega) \cdot (7 - 2\omega) \mu} \right)^{1/2} \quad (15)$$

$$\mu = \mu_{ref} \cdot \left(\frac{T}{T_o} \right)^\omega \quad (16)$$

161 Validation of RGTFun

162 RGTFun is validated across four levels of fidelity: (1) a single-collision analytic benchmark
 163 by comparing Coulomb scattering angles against the exact classical solution; (2) a screened-
 164 potential benchmark by comparing ZBL scattering angles to the Biersack “Magic Formula”
 165 ([Biersack & Haggmark, 1980](#)); (3) a cross-tool benchmark by comparing ZBL-based nuclear
 166 stopping cross sections to SRIM results for H-H ([J. Ziegler, 1985](#)) ([James F. Ziegler et al.,](#)
 167 [2010](#)); and (4) an end-to-end macroscopic benchmark by comparing predicted argon viscosity
 168 and self-diffusion coefficients to NIST reference data ([Kestin et al., 1984](#)).

169 The corresponding validation cases are:

- 170 ■ Coulomb scattering angle: RGTFun vs exact classical solution.
- 171 ■ ZBL scattering angle: RGTFun vs the Magic Formula ([Biersack & Haggmark, 1980](#)).
- 172 ■ Nuclear stopping cross section (H in H): RGTFun (ZBL) vs SRIM ([J. Ziegler, 1985](#))
 173 ([James F. Ziegler et al., 2010](#)).
- 174 ■ Argon transport: viscosity and self-diffusion coefficients vs NIST reference data ([Kestin](#)
 175 et al., 1984).

176 Validation of Rutherford Scattering

177 As a first step in validation, we compared the scattering angle data obtained from RGTFun for
 178 a H-H Coulomb potential to the exact scattering angles for a Coulomb potential ([Goldstein et](#)
 179 [al., 2008](#)). This validation case was chosen because the Coulomb potential is one of the few
 180 potentials for which there exists an exact solution for the scattering angle (the other being the
 181 series solution for the inverse power law potential). This comparison is shown in [Figure 1](#). In
 182 the figure, it is clear that the RGTFun scattering angle calculation is in agreement with the
 183 analytical calculation of Rutherford scattering.

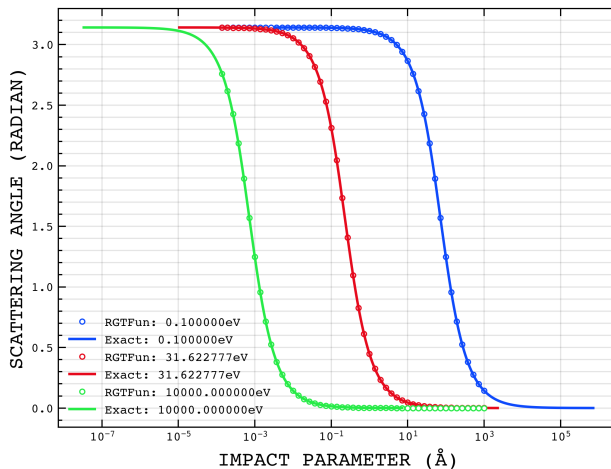


Figure 1: Comparison of scattering angle vs impact parameter curves for three different CM energies for a H-H Coulomb potential. The exact scattering angle curves are plotted as solid lines and the RGTfun scattering angle data are plotted as circles.

184 Validation Against Magic Formula Scattering

185 Next, we compared the scattering angle data obtained from RGTfun for a H-H ZBL potential
 186 to the scattering angle data obtained from the Magic Formula (Biersack & Haggmark, 1980).
 187 This comparison is shown in [Figure 2](#). In the figure, it is clear that the RGTfun scattering
 188 angle calculations are in agreement with the Magic formula. However, RGTfun is slightly more
 189 accurate than the Magic Formula because it calculates the full scattering integral. RGTfun
 190 can also handle a wider range of intermolecular potentials as well as help calculate transport
 191 properties.

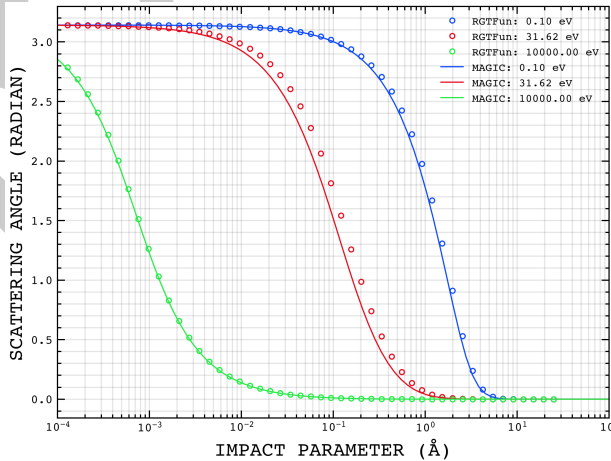


Figure 2: Comparison of scattering angle vs impact parameter curves for three different CM energies for a H-H ZBL potential. The Magic Formula scattering angle curves are plotted as solid lines and the RGTfun scattering angle data are plotted as circles. RGTfun has the advantage of being slightly more accurate than the Magic algorithm as well as being able to handle a wider range of intermolecular potential types.

192 Validation Against SRIM Nuclear Stopping Cross Section

193 Next, we compared the nuclear stopping cross section data obtained from RGTfun for a H-H
 194 ZBL potential to the nuclear stopping cross section data obtained from SRIM (James F. Ziegler

195 et al., 2010). This comparison is shown in Figure 3. In the figure, it is clear that the RGTFun
 196 nuclear stopping cross sections are in excellent agreement with the SRIM nuclear stopping
 197 cross sections.

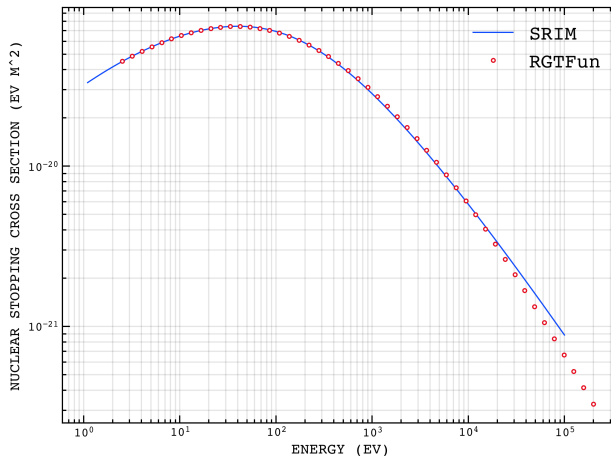


Figure 3: Comparison of RTGFun nuclear stopping cross section data to SRIM nuclear stopping cross section data for H into H. The SRIM data are plotted as solid lines and the RGTFun data are plotted as circles.

198 Validation Against NIST Transport Coefficient Data

199 Lastly, we compared the viscosity and self-diffusion coefficient data obtained from RGTFun
 200 for a 12-6 LJ potential of Ar to NIST transport coefficient data (Kestin et al., 1984). This
 201 comparison is shown in Figure 4 and Figure 5. From the figures we see excellent agreement
 202 between the RGTFun and NIST data for low temperatures, with the curves slightly diverting in
 203 both cases for high temperatures. This diversion is not an error in the calculation, but instead
 204 due to the limitation of the Lennard-Jones potential. This is deduced as the code calculated
 205 the same numerical result as the work of (Khrapak, 2014).

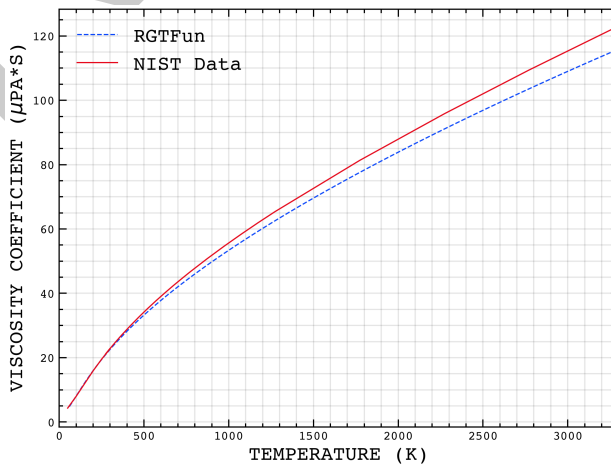


Figure 4: Comparison of RTGFun viscosity coefficient data to NIST viscosity coefficient data for Argon. The NIST data are plotted as a solid line and the RGTFun data are plotted as a dashed line.

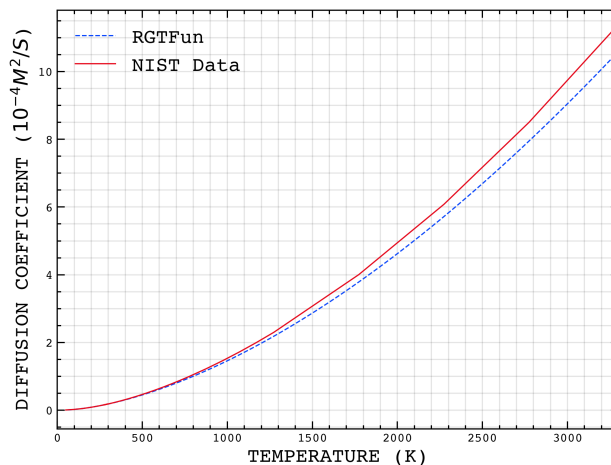


Figure 5: Comparison of RTGFun self-diffusion coefficient data to NIST self-diffusion coefficient data for Argon. The NIST data are plotted as a solid line and the RGTFun data are plotted as a dashed line.

206 Accessing RGTFun

207 RGTFun can be downloaded from the public Github repository linked here:
 208 <https://github.com/nbb2/rgtfun/tree/paper>
 209 Please download all folders from the repository and ensure that they are all located within a
 210 *RGTFun* folder on your machine (it does not have to be called *RGTFun*). This is important
 211 because the app will ask you to select the RGTFun folder on your machine so it can establish
 212 the path to the *src* and *gui* folders. It does not matter where your *RGTFun* folder is located
 213 as long as it is a local folder, i.e. not in a cloud service. Once downloading the repository
 214 folders, you can start the app by opening the *gui.mlapp* file in the *gui* folder.

215 AI Usage Disclosure

216 ChatGPT (OpenAI; model: GPT-5.2 Thinking) was used to assist with paper text (wording,
 217 structure, clarity) during drafting. Assistance was limited to editorial support: suggesting
 218 alternative phrasing and tightening paragraphs. We did not use AI to generate the core
 219 scientific/technical claims, results, or validation data. All AI-assisted suggestions were reviewed,
 220 edited, and validated by the authors. The authors made all core design decisions, verified
 221 technical accuracy, and take full responsibility for the content, originality, and correctness of
 222 the manuscript and associated software.

223 References

- 224 Amdur. (1961). An experimental approach to the determination of gaseous transport properties
 225 at very high temperatures. *Planetary and Space Science*, 3, 228–235. [https://doi.org/10.1016/0032-0633\(61\)90250-1](https://doi.org/10.1016/0032-0633(61)90250-1)
- 227 Amdur, I. (1949). Repulsive Interaction Potentials at Small Interaction Distances: He–He and
 228 H–H₂ Systems. *The Journal of Chemical Physics*, 17(9), 844–845. <https://doi.org/10.1063/1.1747419>
- 230 Amdur, I., & Harkness, A. L. (1954). Scattering of High-Velocity Neutral Particles. II. Helium–
 231 Helium. *The Journal of Chemical Physics*, 22(4), 664–669. <https://doi.org/10.1063/1.1740144>

- 233 Biersack, J. P., & Haggmark, L. G. (1980). A Monte Carlo computer program for the transport
234 of energetic ions in amorphous targets. *Nuclear Instruments and Methods*, 174(1-2),
235 257–269. [https://doi.org/10.1016/0029-554X\(80\)90440-1](https://doi.org/10.1016/0029-554X(80)90440-1)
- 236 Bird, G. A. (2013). *The DSMC method* (Version 1.2). G. A. Bird. ISBN: 978-1-4921-1290-7
- 237 Chapman, S., & Cowling, T. G. (1990). *The mathematical theory of non-uniform gases: An*
238 *account of the kinetic theory of viscosity, thermal conduction, and diffusion in gases* (3rd
239 ed.). Cambridge University Press. ISBN: 978-0-521-40844-8
- 240 Fratus, K. (2015). *Scattering*. <https://web.physics.ucsb.edu/~fratus/phys103/LN/Scattering.pdf>
- 241
- 242 Goldstein, H., Poole, C. P., & Safko, J. L. (2008). *Classical mechanics* (3. ed., [Nachdr.]).
243 Addison Wesley. ISBN: 978-0-201-65702-9
- 244 Janssen, J. (2018). *MagnumPI*. <https://gitlab.com/magnumpi/magnumpi>.
- 245 Kestin, J., Knierim, K., Mason, E. A., Najafi, B., Ro, S. T., & Waldman, M. (1984). Equilibrium
246 and Transport Properties of the Noble Gases and Their Mixtures at Low Density. *Journal of*
247 *Physical and Chemical Reference Data*, 13(1), 229–303. <https://doi.org/10.1063/1.555703>
- 248 Khrapak, S. A. (2014). Accurate transport cross sections for the Lennard-Jones potential. *The*
249 *European Physical Journal D*, 68(10), 276. <https://doi.org/10.1140/epjd/e2014-50449-y>
- 250 Lane, G. H., & Everhart, E. (1960). Calculations of Total Cross Sections for Scattering
251 from Coulomb Potentials with Exponential Screening. *Physical Review*, 117(4), 920–924.
252 <https://doi.org/10.1103/PhysRev.117.920>
- 253 Lennard-Jones, J. E. (1931). Cohesion. *Proceedings of the Physical Society*, 43(5), 461.
- 254 Maitland, G. C. (Ed.). (1987). *Intermolecular forces: Their origin and determination* (Repr.).
255 Clarendon Pr. ISBN: 978-0-19-855641-1
- 256 Morse, P. M. (1929). Diatomic molecules according to the wave mechanics. II. Vibrational
257 levels. *Physical Review*, 34(1), 57.
- 258 Ruzic, D. N., & Cohen, S. A. (1984). Total scattering cross sections and interatomic potentials
259 for neutral hydrogen and helium on some noble gases. *Journal of Chemical Physics*, 83,
260 5527–5530. <https://api.semanticscholar.org/CorpusID:97010285>
- 261 Valiev, M., Bylaska, E. J., Govind, N., Kowalski, K., Straatsma, T. P., Van Dam, H. J. J.,
262 Wang, D., Nieplocha, J., Apra, E., Windus, T. L., & De Jong, W. A. (2010). NWChem:
263 A comprehensive and scalable open-source solution for large scale molecular simulations.
264 *Computer Physics Communications*, 181(9), 1477–1489. <https://doi.org/10.1016/j.cpc.2010.04.018>
- 265
- 266 Zhen, S., & Davies, G. (1983). Calculation of the lennard? Jones n? M potential energy
267 parameters for metals. *Physica Status Solidi (a)*, 78(2), 595–605.
- 268 Ziegler, J. (1985). *Treatise on Heavy-Ion Science: Volume 6: Astrophysics, Chemistry, and*
269 *Condensed Matter*. Springer International Publishing. ISBN: 978-1-4615-8103-1
- 270 Ziegler, J. F., Biersack, J. P., & Littmark, U. (1983). *EMPIRICAL STOPPING*
271 *POWERS FOR IONS IN SOLIDS*. (pp. 1861–1873) [Conference paper]. <https://www.scopus.com/inward/record.uri?eid=2-s2.0-0020977537&partnerID=40&md5=971582a2ffcd613de36454248045b650>
- 272
- 273
- 274 Ziegler, James F., Ziegler, M. D., & Biersack, J. P. (2010). SRIM – The stopping and
275 range of ions in matter (2010). *Nuclear Instruments and Methods in Physics Research*
276 *Section B: Beam Interactions with Materials and Atoms*, 268(11-12), 1818–1823. <https://doi.org/10.1016/j.nimb.2010.02.091>
- 277